CONFIDENTIAL

Copy 197
RM E55H16a

HOLLOMAN AIR FORCE BASE
ALBUQUERQUE, NEW MEXICO

TECH LIBRARY KAFB, NM
0144053

NACA RM E55H16a

6533

NACA

RESEARCH MEMORANDUM

EFFECT OF CENTERBODY BOUNDARY-LAYER REMOVAL NEAR THE THROAT OF THREE CONICAL NOSE INLETS AT MACH 1.6 TO 2.0

By Emil J. Kremzier and George A. Wise

Lewis Flight Propulsion Laboratory
Cleveland, Ohio

(Unclassified)
NASA Tech Pub Announcement #11
(OFFICER AUTHORIZED TO CHANGE)
21 Jan 60
NJC
(OFFICER MAKING CHANGE)
24 Feb. 61
DATE
CLASSIFIED DOCUMENT

This material contains information affecting the National Defense of the United States within the meaning of the espionage laws, Title 18, U.S.C., Secs. 793 and 794, the transmission or revelation of which in any manner to an unauthorized person is prohibited by law.

NATIONAL ADVISORY COMMITTEE FOR AERONAUTICS

WASHINGTON

November 15, 1955

CONFIDENTIAL

TECH LIBRARY KAFB, NM
0144053

 [redacted]

NATIONAL ADVISORY COMMITTEE FOR AERONAUTICS

RESEARCH MEMORANDUM

EFFECT OF CENTERBODY BOUNDARY-LAYER REMOVAL NEAR THE THROAT OF THREE CONICAL NOSE INLETS AT MACH 1.6 TO 2.0

By Emil J. Kremzier and George A. Wise

3833

CD-1

SUMMARY

An experimental investigation of the effect of compression surface boundary-layer bleed near the throat of three full-scale conical nose inlets was conducted in the Lewis 8- by 6-foot supersonic wind tunnel at zero angle of attack for a Mach number range of 1.6 to 2.0.

Inlet critical and peak pressure recoveries were increased by bleeding off the spike-surface boundary layer. However, no gain in propulsion-system thrust minus drag was realized for a hypothetical turbojet installation, because the pressure-recovery increase was too small to compensate for the estimated bleed system drag. The bleed system was effective in removing the low-energy air near the surface of 25° and 30° half-angle spikes and in reducing the amount of low-energy air near the surface of a 20° spike. With no bleed, distortion of the diffuser-discharge total-pressure profile was less than the profile distortion near the throat as a result of flow mixing in the subsonic diffuser. Profile peaks at the diffuser discharge were shifted toward the centerbody when the bleed was opened, and no significant difference in the amount of distortion was noted. The range of stable inlet operation was generally decreased by operation of the bleed system.

INTRODUCTION

Efficient supersonic-inlet performance is often impaired by the presence of boundary layer on the inlet compression surface. The interaction of this boundary layer with the inlet terminal shock may result in large regions of low-energy air entering the inlet with attendant losses in pressure recovery, distortion of diffuser-discharge total-pressure profiles, and inlet instability. Removal of the compression surface boundary layer by means of slots or scoops near the throat of ramp-type inlets has been investigated (refs. 1 and 2). Substantial gains in pressure recovery were noted. An effect of type and amount of boundary-layer removal on inlet stability and diffuser-discharge

 [redacted]

total-pressure distribution is also indicated (ref. 1). Boundary-layer removal ahead of the cowl lip increased both the stable range and pressure recovery of a conical nose inlet (ref. 3).

Because of the promising results of compression surface boundary-layer bleed, a further investigation of the effect of bleed on the performance of three conical nose inlets was conducted. Full-scale inlets with conical centerbodies perforated near the throat were investigated for a range of Mach numbers from 1.6 to 2.0. Three different cone angles were tested over a range of inlet mass-flow ratios with and without boundary-layer bleed. The investigation was conducted in the Lewis 8- by 6-foot supersonic wind tunnel. 3833

SYMBOLS

The following symbols are used in this report:

A flow area, sq ft

A_c inlet capture area

M Mach number

M_D design Mach number, Mach number at which conical shock intersects cowl lip

m_B bleed mass flow

m_0 free-stream mass flow

m_4 main duct mass flow

$\frac{m_4}{m_0}$ mass-flow ratio, $\frac{\rho_4 V_4 A_4}{\rho_0 V_0 A_c}$

P total pressure

p static pressure

V velocity

θ spike half-angle

ρ mass density

Subscripts:

l local condition

0 free-stream

3 diffuser discharge, station 64.5 for 20° spike and station 62.5 for 25° and 30° spike

4 mass-flow survey, station 124.5 for 20° spike and station 122.5 for 25° and 30° spike

Pertinent areas:

A_c 1.62 sq ft (20° spike); 1.66 sq ft (25° and 30° spike)

A_3 2.08 sq ft

A_4 2.93 sq ft

APPARATUS AND PROCEDURE

A schematic drawing of the model is shown in figure 1. The model is similar to the cold-flow model of reference 4, incorporating the same support system, mass-flow control plug, and translating spike. However, the bypass system was modified so that the centerbody could be evacuated through three hollow struts by opening the bypass door. Boundary layer was bled into the evacuated centerbody through perforations in the spike surface near the inlet throat, just inside the cowl lip. Three spikes with cone half-angles of 20°, 25°, and 30°, respectively, were investigated. A photograph of the perforated spikes is presented in figure 2, and location and distribution of the perforations are shown in figure 3. Subsonic-diffuser-area variations for the three spike configurations are presented in figure 4 for the extreme rearward (design Mach number M_D, 1.6) and forward (M_D, 2.0) spike positions. Area variations for only the first 28 inches of diffuser length are presented for the 25° and 30° spikes, since all three configurations were identical downstream of this station. For the 20° spike, the cowl lip was extended forward 2 inches to maintain a suitable range of inlet design Mach number M_D. Because of this cowl extension, corresponding diffuser stations for the 20° spike are increased 2 inches over those for the 25° and 30° spike, where the original cowl of reference 4 was used. Unless otherwise specified, model stations will be discussed in terms of distance downstream from the original cowl lip (25° and 30° spikes).

Model instrumentation was installed to measure total and static pressures at station 3 (62.5 in. from cowl lip, fig. 1), and static pressures at station 4 (122.5 in. from cowl lip, fig. 1). A boundary-layer rake was mounted on the spike surface just behind the perforated region, and four bleed mass-flow metering nozzles were located inside the hollow centerbody downstream of the perforated region. Static-pressure orifices were located at the throat of each nozzle to determine the bleed mass-flow ratio m_B/m_0.

3833 back CQ-1

Diffuser-discharge total pressure P_3 was obtained from an area-weighted average of the total-pressure readings at station 3. The mass-flow ratio m_4/m_0 was calculated from the Mach number M_4 and the average static pressure p_4. The Mach number M_4 was obtained from the calibrated area ratio between station 4 and the choked exit plug. Inlet pulsing was detected by a pressure transducer at station 3 and by observation of the schlieren apparatus.

Spike positions of $M_D = M_0$ and $M_D = 2.0$ were investigated in the Lewis 8- by 6-foot supersonic wind tunnel for a range of free-stream Mach numbers from 1.6 to 2.0. Data were taken with and without center-body bleed for each spike angle tested. The model was run at zero angle of attack for a range of inlet mass-flow ratios. Reynolds number for the investigation varied from about 5.3×10^6 to 5.9×10^6 per foot of length. 3833

RESULTS AND DISCUSSION

Inlet Pressure Recovery

Variation of diffuser-pressure recovery with inlet mass-flow ratio is shown in figures 5(a), (b), and (c) for free-stream Mach numbers of 1.6, 1.8, and 2.0, respectively. In all cases where the curves are completely defined, both peak and estimated critical pressure recoveries are increased with spike boundary-layer bleed. For a M_D of 1.6, supercritical inlet operation was not attainable because of the limitation on the available open exit area (fig. 5(a)). In general, the pressure recovery for subcritical inlet operation is increased when the bleed is opened. At free-stream Mach numbers of 1.6 and 1.8 (figs. 5(a) and (b)), peak pressure recoveries were higher at $M_D = 2.0$ (oblique shock ahead of lip at Mach numbers below 2.0) than at $M_D = M_0$ (oblique shock on lip) with bleed open or closed. Bleed mass flow decreases as the inlet terminal shock passes downstream over the perforated region (ref. 5). Supercritical inlet operation is defined herein as operation with the inlet terminal shock inside the cowl lip (constant mass-flow ratio at the cowl-lip station). For the bleed-open case, the mass-flow ratio m_4/m_0 for the upper supercritical portion of the curves increases with decreasing diffuser back pressure. Maximum bleed mass-flow ratio m_B/m_0 within the inlet stable operating range varied from about 0.06 to 0.08 for subcritical inlet operation.

Theoretical bleed-drag estimates were made so that a propulsion-system thrust minus incremental bleed drag could be determined for a typical turbojet installation. The bleed was assumed to have a sonic axial discharge with a pressure recovery equal to that of the inlet. This assumption results in optimistic values of bleed drag, since the

bleed system obviously has a lower pressure recovery than that of the inlet. Even though the bleed-drag estimates were optimistic, no gain in propulsion-system thrust minus incremental drag was realized with boundary-layer bleed. This result contrasts with those of references 1 and 2 for ramp-type inlets, where increases in thrust minus drag were obtained with ramp boundary-layer bleed.

Diffuser Total-Pressure Profiles

3833

The total-pressure profile distortions observed at the subsonic diffuser discharge reflect distortions of the inlet entrance flow to a large extent. Schlieren observations indicate the formation of a lambda shock on the spike surface ahead of the cowl lip with attendant boundary-layer thickening or separation, as shown in the following sketch:

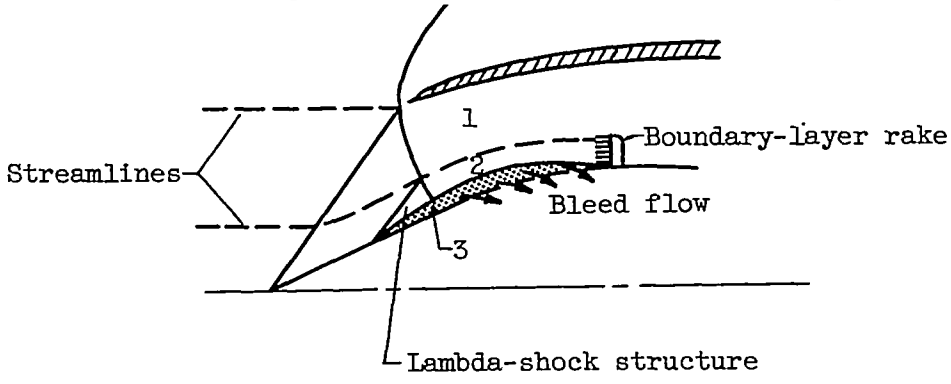

For these inlets, the entrance flow may be divided into the three possible regions shown in the sketch: (1) the high-energy portion of the flow outside the lambda shock that passed through the main inlet oblique and/or normal shock, (2) the higher-energy portion that passed through the original oblique shock, and the oblique and normal shock associated with the lambda structure, and (3) the low-energy portion associated with the boundary-layer thickening or separation at the base of the lambda structure. As the cone angle increases, the extent of regions (2) and (3) decreases. A schlieren photograph of the 20° inlet at near critical operation is shown in figure 6 for $M_D = M_0 = 2.0$. Part of the lambda-shock structure is visible ahead of the cowl lip on the upper surface of the spike. Asymmetry of the inlet shock structure in the photograph may have been caused by a small amount of spike eccentricity on the model.

These qualitative observations of the inlet flow regions are substantiated by the internal radial total-pressure profiles presented in figure 7. The data were obtained at the inlet operating points indicated by the solid symbols of figure 5(c). The left-hand set of curves shows the total-pressure profiles obtained with a boundary-layer rake immediately downstream of the perforations. For the 20° spike with the bleed

closed (fig. 7(a)), a large region of low-energy air extends out beyond the height of the rake. With the bleed open, the total-pressure level is increased, and the value at the outer end of the rake approaches the theoretical pressure recovery at the cone surface. Since this total-pressure level is still below the theoretical value, it may be concluded that the low-energy portion of the air has not been completely removed.

For the 25° spike (fig. 7(b)), opening the bleed removes essentially all of the low-energy air on the spike surface. The high total-pressure ratio region extending to about 10 percent of the duct height is greater than the theoretical value of 0.92 across one oblique and one normal shock. This region is believed to represent the higher-energy portion of the flow in region (2) of the sketch. 3833

Low-energy air near the spike surface is least extensive for the 30° spike, covering about 15 percent of the duct height with the bleed closed (fig. 7(c)). Again, opening the bleed removes virtually all of the low-energy air. No total-pressure ratios higher than theoretical are obtained for this inlet, indicating negligible or nonexistent lambda-shock effects.

Profiles at the diffuser discharge (right-hand set of curves in fig. 7) were measured with two diametrically opposite rakes located to avoid strut wakes. Axial symmetry was indicated. With the bleed closed, the large distortions observed at the diffuser entrance were reduced considerably at the discharge station, as a result of flow mixing in the subsonic diffuser. The improvement in throat profiles by the use of boundary-layer removal correspondingly improved the pressure recovery near the centerbody at the discharge. However, the amount of distortion at the diffuser discharge was not significantly changed.

Inlet Stability

Stability limits of the three inlets investigated are presented in figure 8 for the free-stream Mach number range of the tests. The total mass-flow ratio shown on the ordinate includes the bleed mass flow m_B and represents the total mass-flow ratio entering the cowl lip.

Except for the 20° spike inlet at $M_D = M_0$, the range of stable inlet operation is decreased when the bleed is opened. This destabilizing effect becomes more pronounced with increasing spike angle (fig. 8). Investigation of two other conical nose inlets showed substantial increases in the range of stable operation with spike bleed (refs. 5 and 6). However, the spike bleed for these inlets was located ahead of the cowl lip. Whether relocation of the bleed for the present inlet would increase the stable range is unknown.

For bleed closed, increasing the spike angle increases the maximum free-stream Mach number for completely stable inlet operation. Maximum Mach number for complete stable operation is also greater for spike positions of $M_D = M_0$ than for $M_D = 2.0$ with bleed open or closed.

SUMMARY OF RESULTS

3833

An experimental investigation of the effect of compression-surface boundary-layer bleed near the throat of three full-scale conical nose inlets was conducted for a Mach number range of 1.6 to 2.0. Bleed mass flows up to 8 percent of inlet mass flows were removed. The following results were obtained:

1. Inlet critical and peak pressure recoveries were increased by bleeding off the spike-surface boundary layer near the throat. No gain in propulsion-system thrust minus drag for a typical turbojet installation was indicated, however, because the increased pressure recovery was more than offset by the bleed system drag.

2. For inlet operation near critical at a free-stream Mach number of 2.0, the spike bleed was effective in removing the low-energy air near the surface of the 25° and 30° spikes. The bleed was also effective in reducing the amount of low-energy air near the surface of the 20° spike.

3. With no bleed, distortion of the diffuser discharge total-pressure profiles was considerably less than the profile distortion near the throat, as a result of flow mixing in the subsonic diffuser. Profile peaks at the diffuser discharge were shifted toward the centerbody when the bleed was opened, and no significant difference in the amount of distortion was noted.

4. Spike bleed generally decreased the range of stable inlet operation. This destabilizing effect became more pronounced with increasing spike angle.

Lewis Flight Propulsion Laboratory
National Advisory Committee for Aeronautics
Cleveland, Ohio, August 23, 1955

REFERENCES

1. Obery, Leonard J., and Cubbison, Robert W.: Effectiveness of Boundary-Layer Removal Near Throat of Ramp-Type Side Inlet at Free-Stream Mach Number of 2.0. NACA RM E54I14, 1954.

2. Campbell, Robert C.: Performance of a Supersonic Ramp Inlet with Internal Boundary-Layer Scoop. NACA RM E54I01, 1954.

3. Obery, Leonard J., Englert, Gerald W., and Nussdorfer, Theodore J.: Pressure Recovery, Drag, and Subcritical Stability Characteristics of Conical Supersonic Diffusers with Boundary-Layer Removal. NACA RM E51H29, 1952.

4. Nettles, J. C., and Leissler, L. A.: Investigation of Adjustable Supersonic Inlet in Combination with J34 Engine up to Mach 2.0. NACA RM E54H11, 1954.

5. Evvard, John C., and Blakey, John W.: The Use of Perforated Inlets for Efficient Supersonic Diffusion. NACA RM E51B10, 1951.

6. Connors, James F., and Meyer, Rudolph C.: Performance Characteristics of Axisymmetric Two-Cone and Isentropic Nose Inlets at Mach Number 1.90. NACA RM E55F29, 1955.

3833

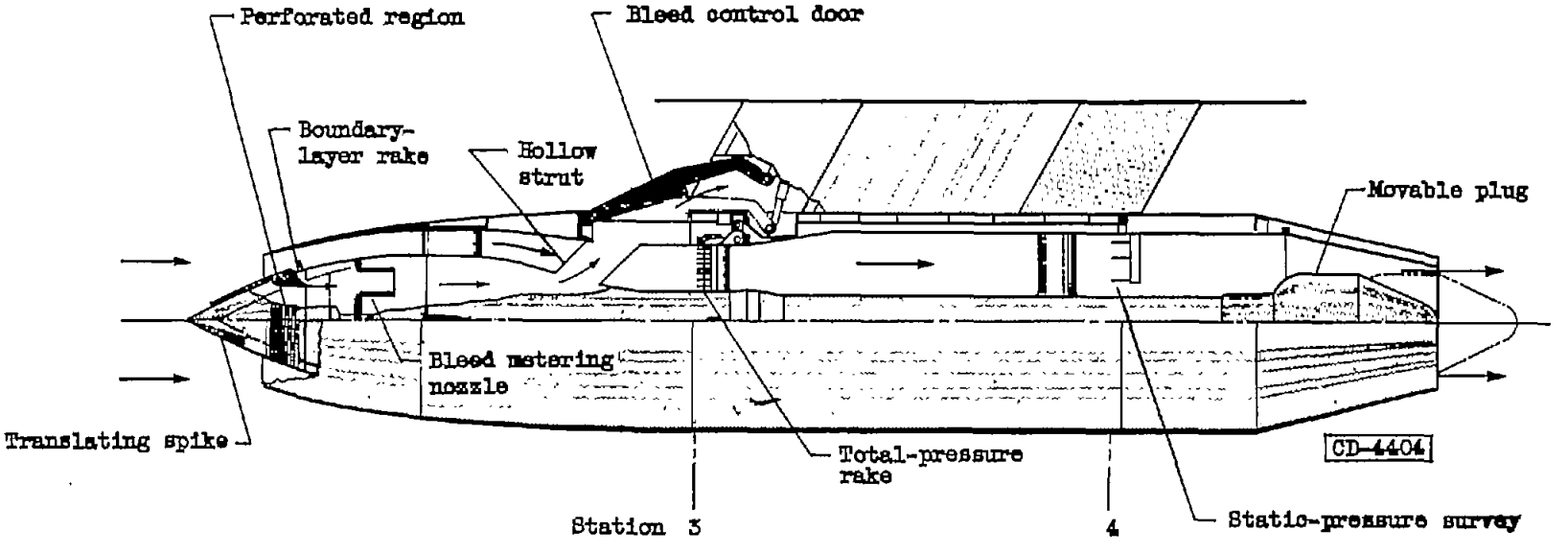

Figure 1. - Schematic of model investigated. Length of model, 164.4 (cowl lip to end of tail pipe); maximum diameter, 30.1; cowl-lip diameter, 17.25 (20° spike), 17.44 (25° and 30° spike). (All dimensions in inches.)

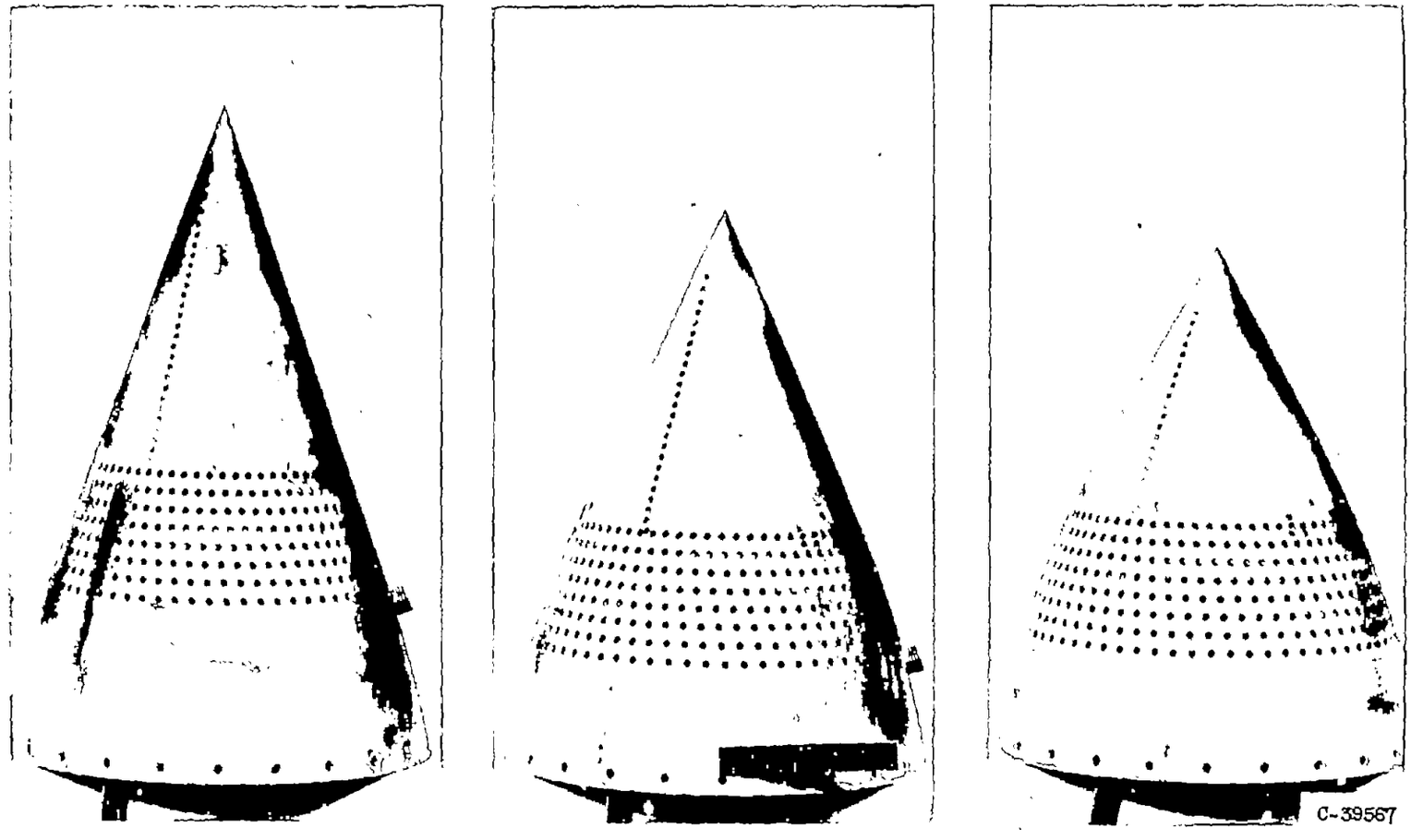

(a) 20° Spike. (b) 25° Spike. (c) 30° Spike.

Figure 2. - Perforated spikes.

CONFIDENTIAL

3833

CD-2 back

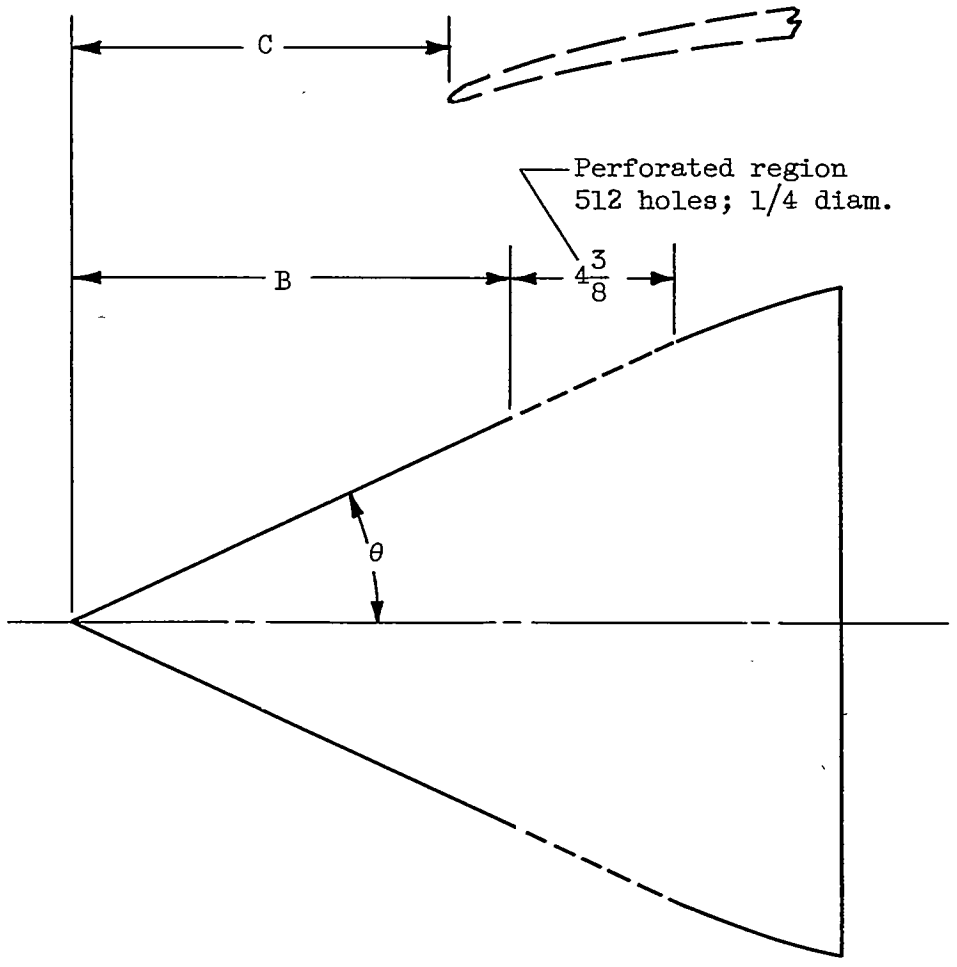

θ, deg	B, in.	C, in., at M_D of		
		1.6	1.8	2.0
20	13.56	8.35	9.94	11.15
25	11.81	7.02	8.30	9.37
30	10.06	5.33	6.83	8.02

Figure 3. - Location and distribution of perforations on conical spike (dimensions in inches). Holes located in eight circumferential rows, 64 holes per row equally spaced, with 5/8 spacing between rows. Each successive row rotated 1° circumferentially, with respect to the previous row, in one consistent direction.

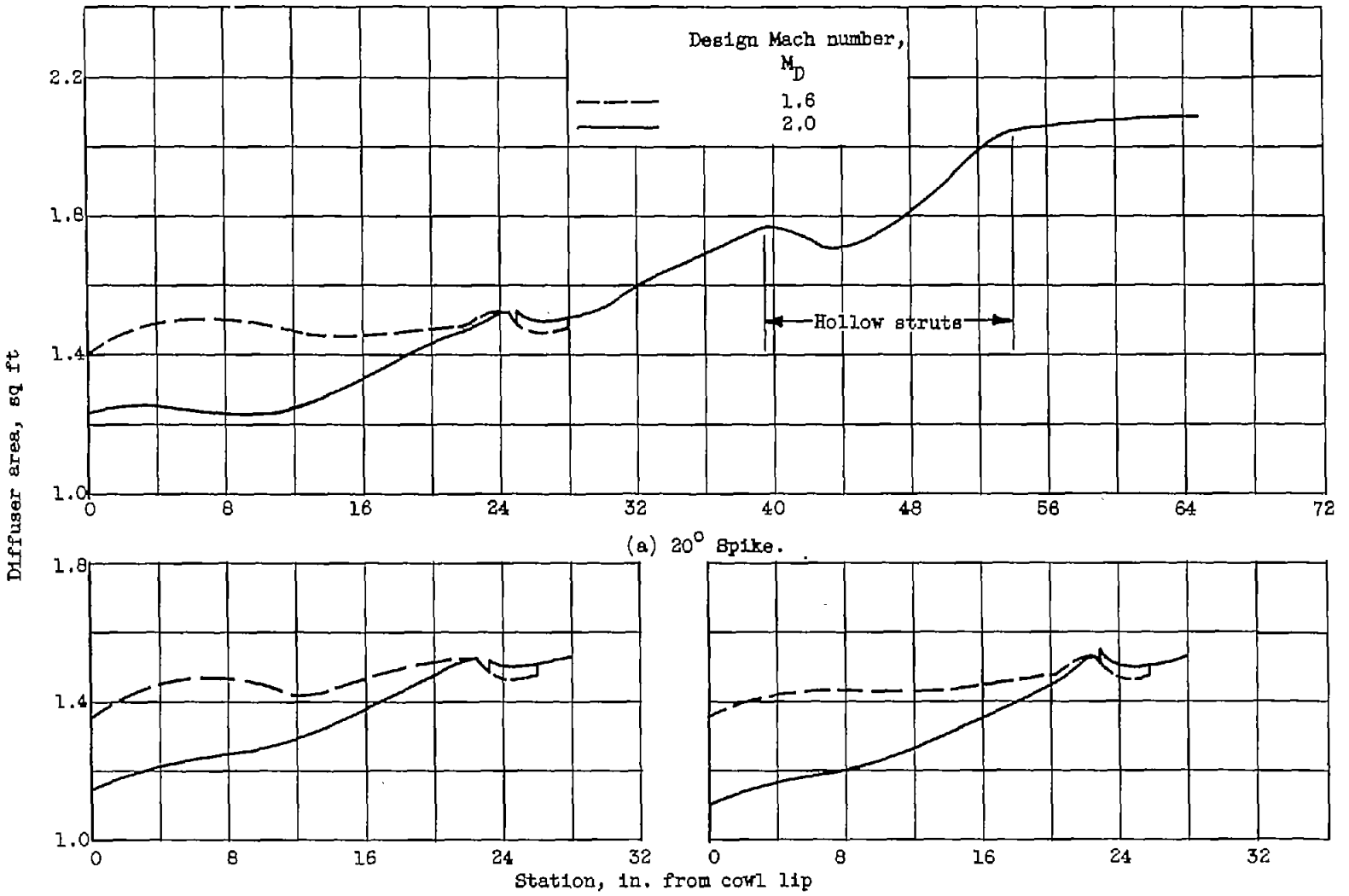

(a) 20° Spike.

(b) 25° Spike.

(c) 30° Spike.

Figure 4. - Subsonic-diffuser-area variations.

CONFIDENTIAL

3833

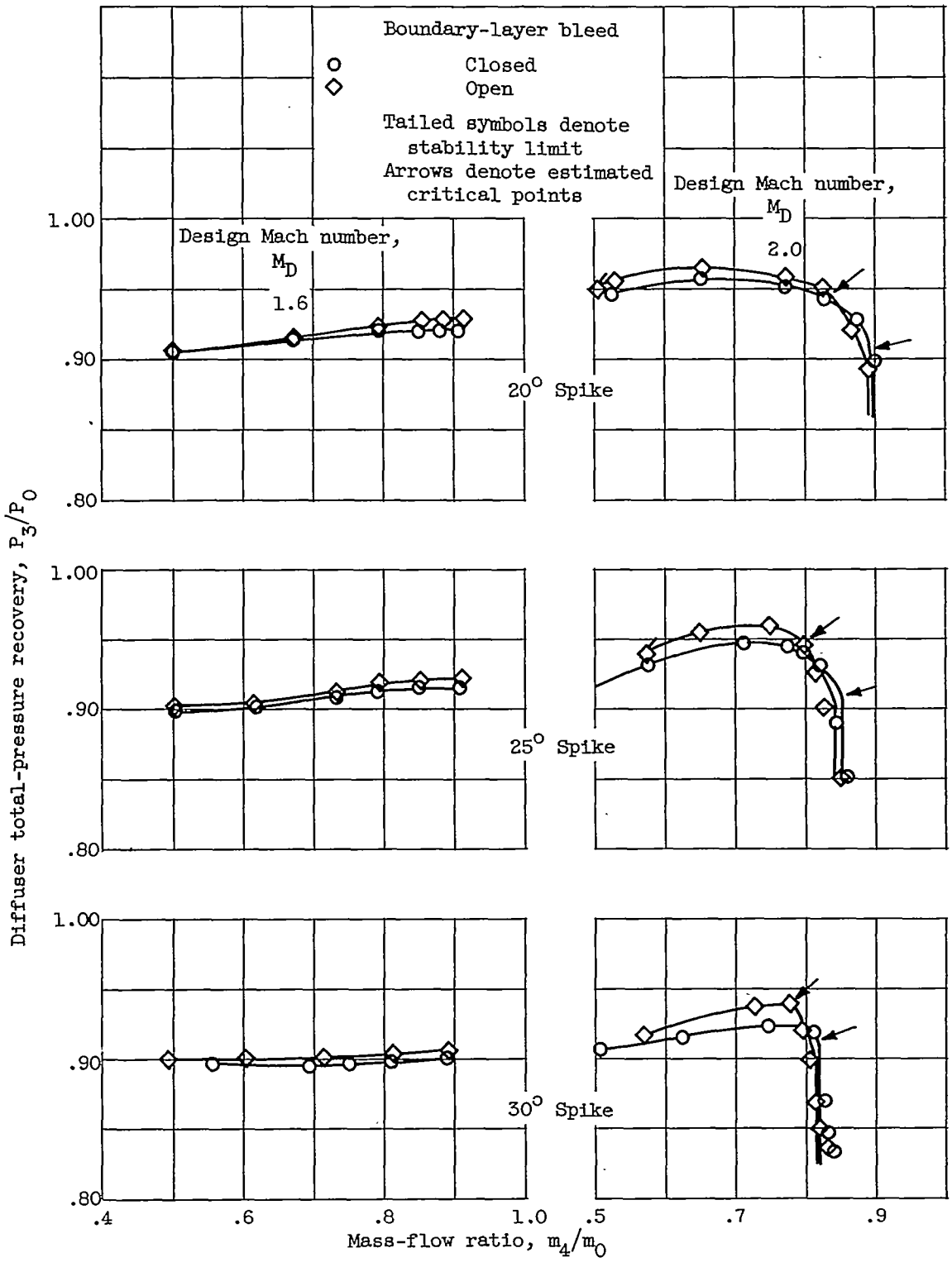

(a) Free-stream Mach number, 1.6.

Figure 5. - Effect of spike bleed on diffuser-pressure recovery.

3833

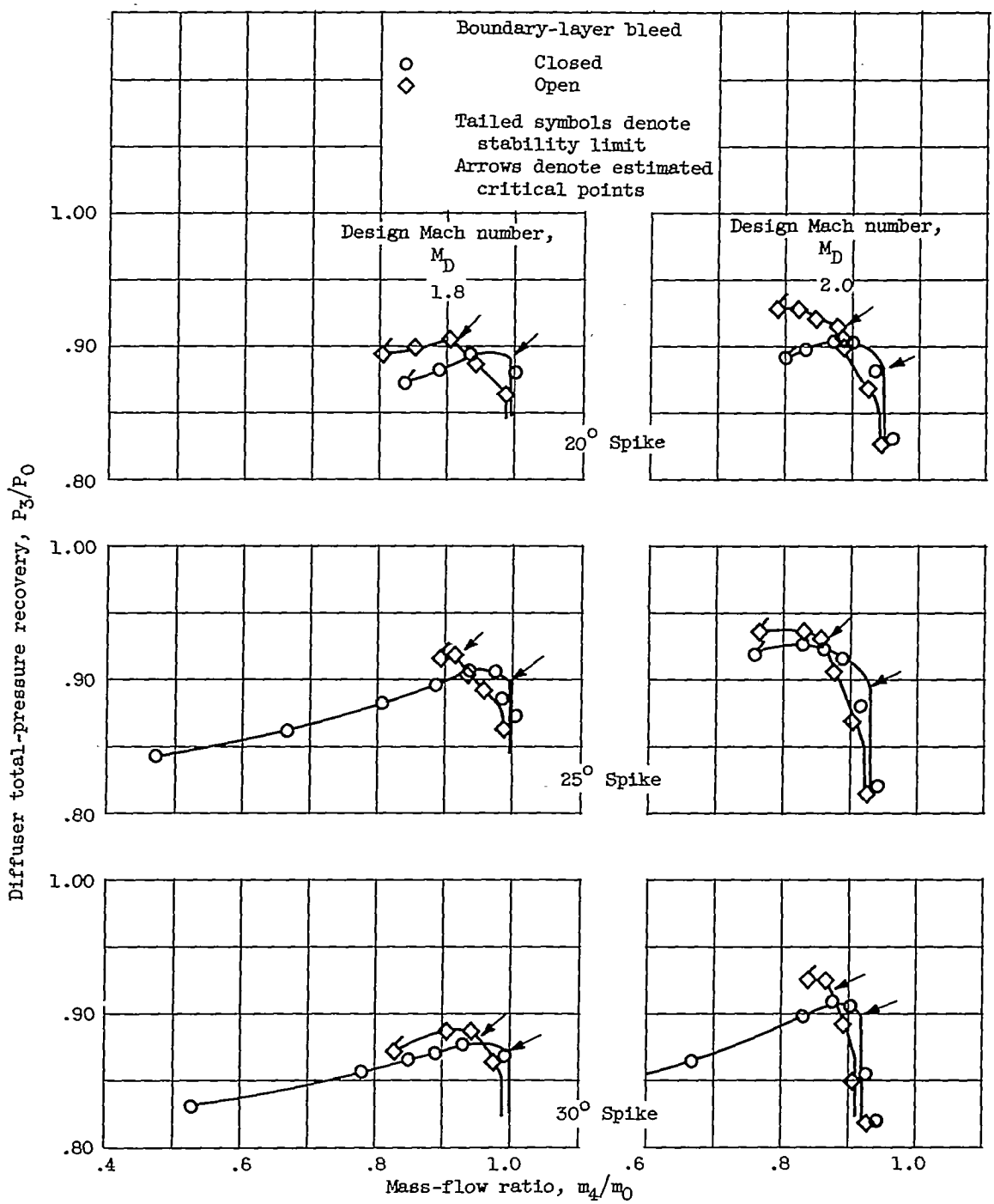

(b) Free-stream Mach number, 1.8.

Figure 5. - Continued. Effect of spike bleed on diffuser-pressure recovery.

3833

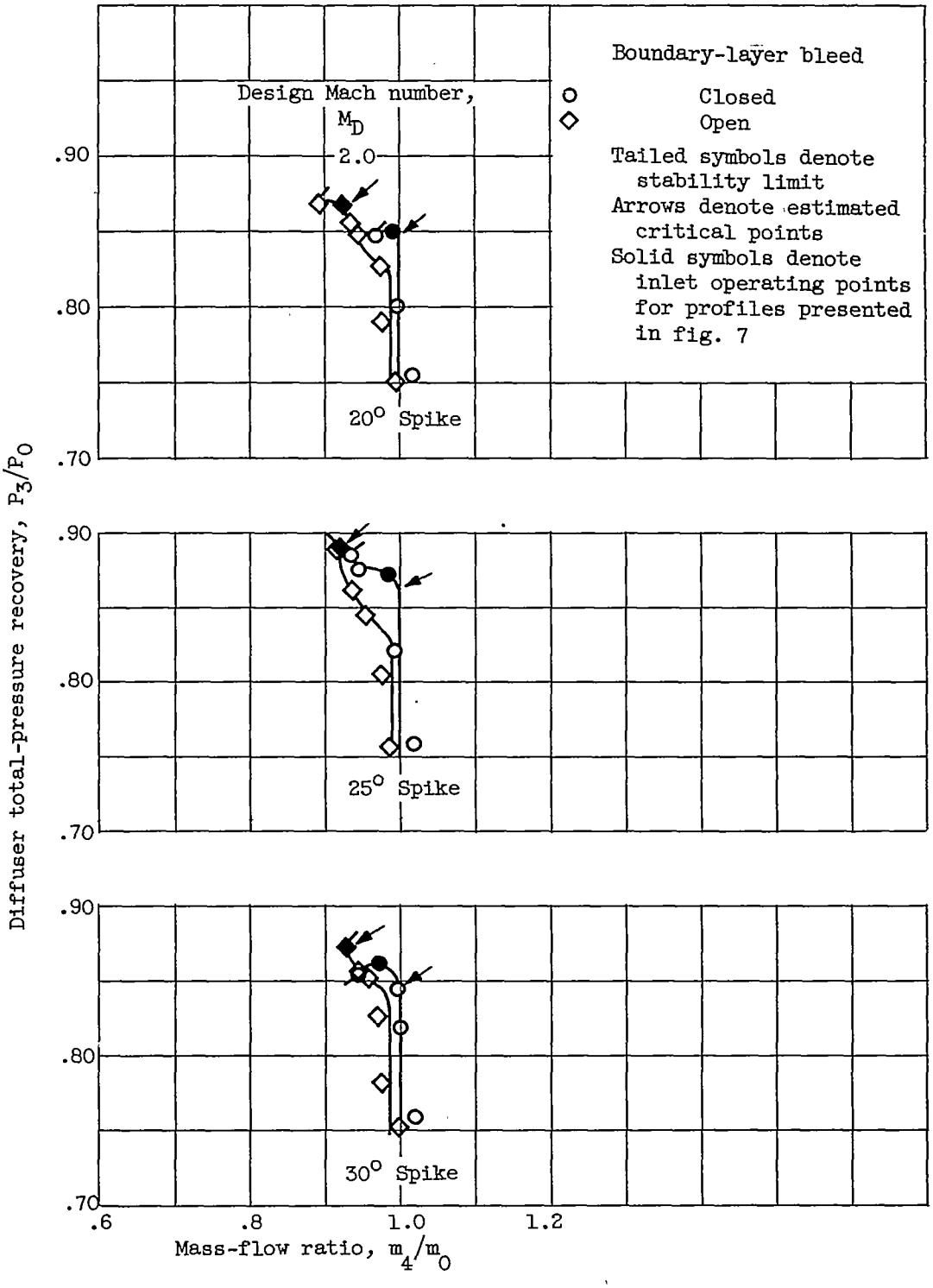

(c) Free-stream Mach number, 2.0.

Figure 5. - Concluded. Effect of spike bleed on diffuser-pressure recovery.

3833

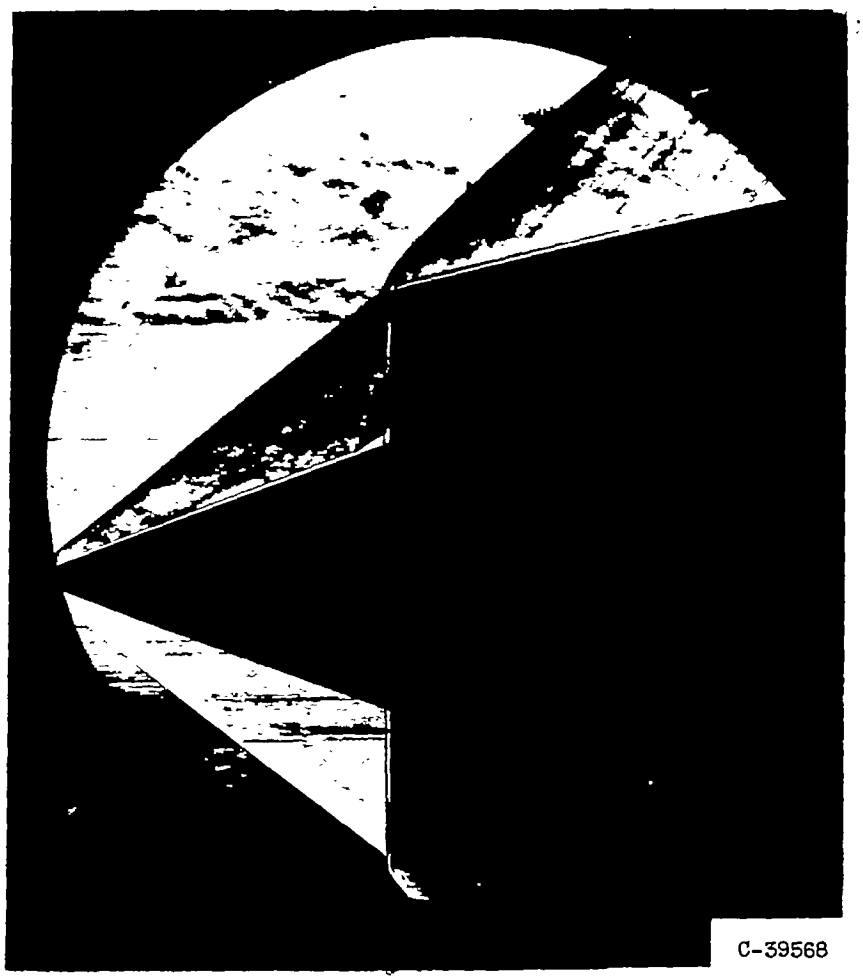

Figure 6. - Schlieren photograph of 20° inlet near critical operation. Bleed closed; design and free-stream Mach numbers, 2.0.

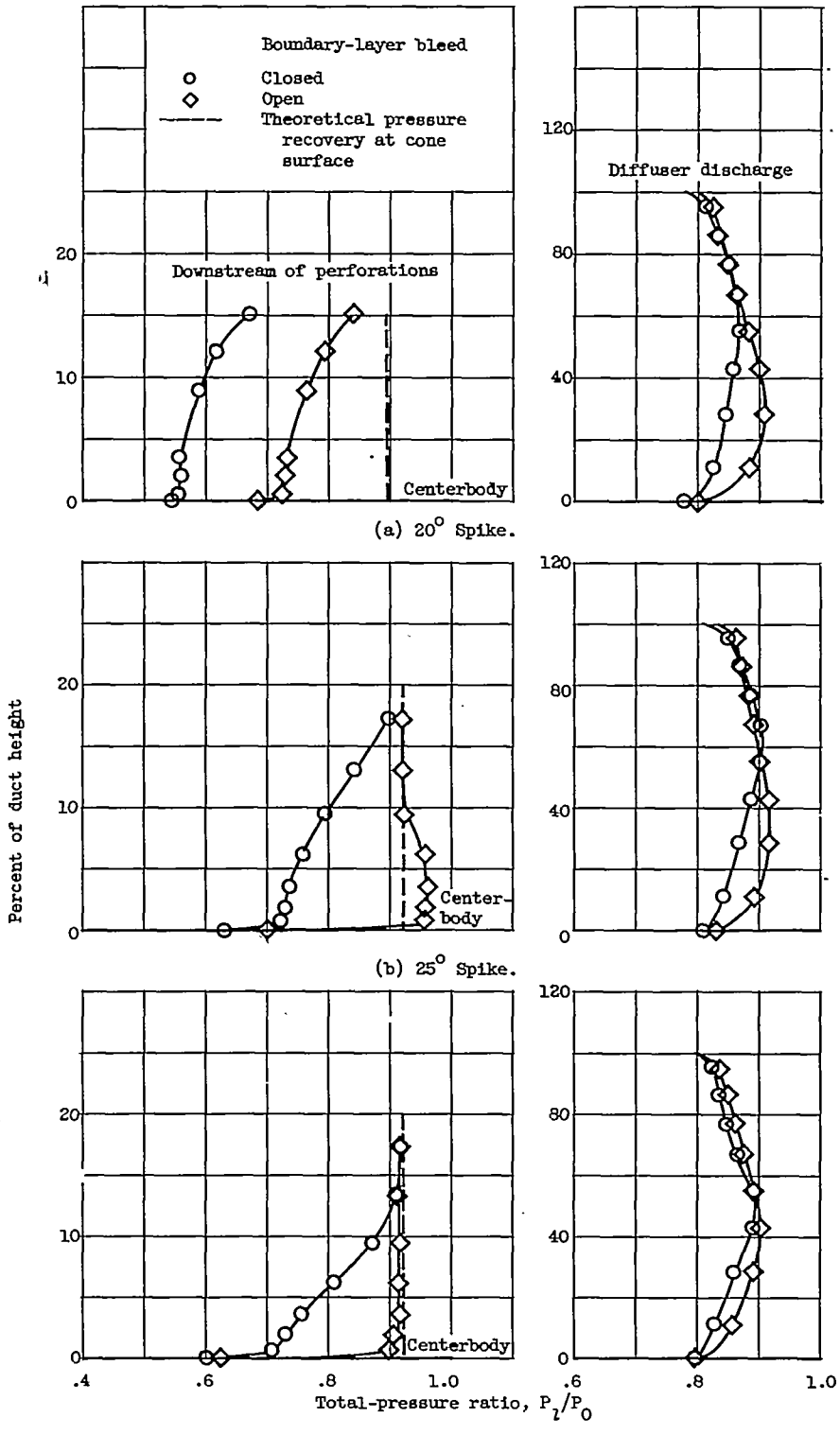

(a) 20° Spike.

(b) 25° Spike.

(c) 30° Spike.

Figure 7. - Effect of spike bleed on diffuser profiles for inlet operation indicated by solid data points of figure 5(c). Design and free-stream Mach numbers, 2.0.

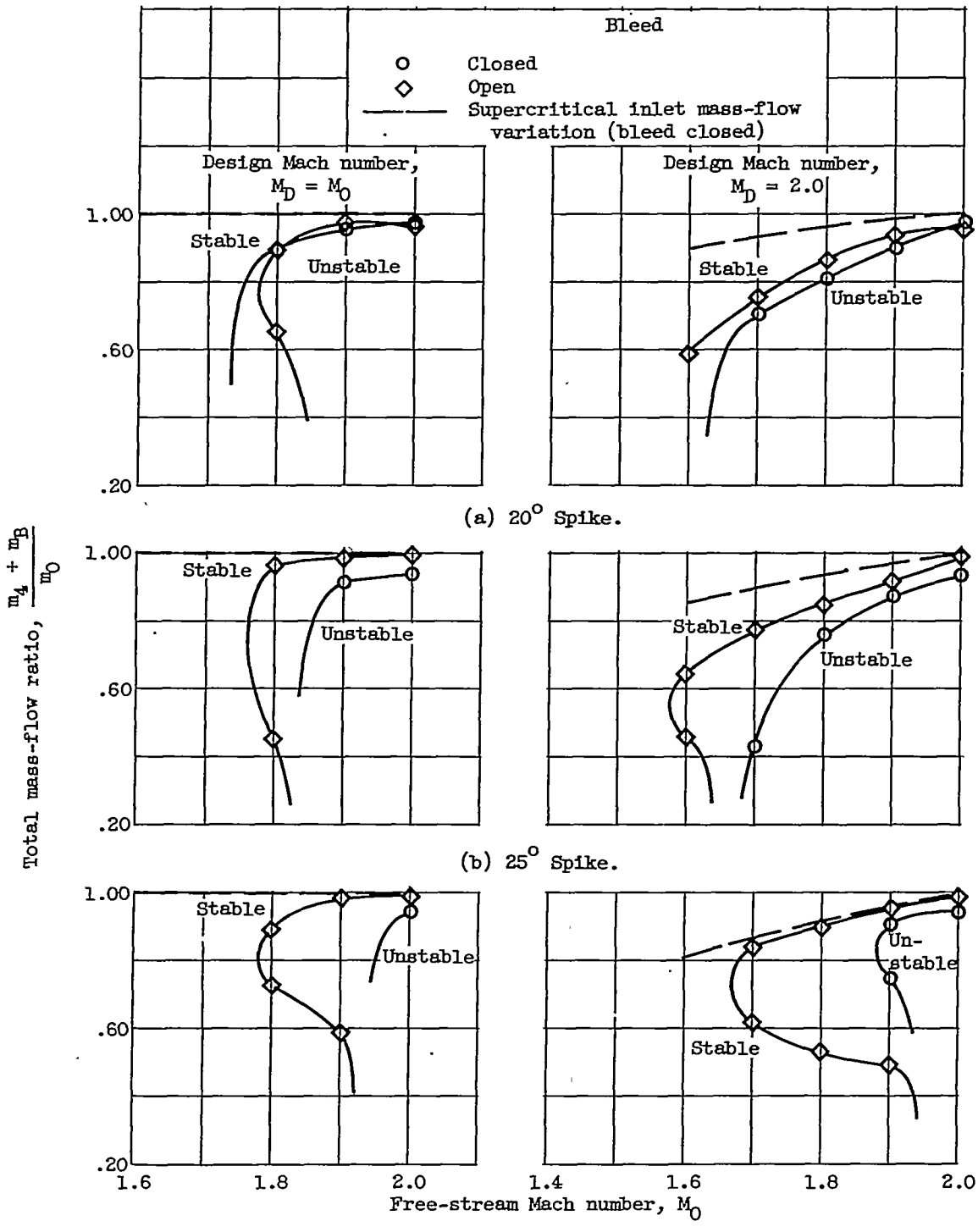

(a) 20° Spike.

(b) 25° Spike.

(c) 30° Spike.

Figure 8. - Inlet stability limits.